Effect of titanium dioxide on chemical and molecular changes in PVC sidings during QUV accelerated weathering

Teng-Chun Yang [a,c], Takafumi Noguchi [a], Minoru Isshiki [b], Jyh-Horng Wu [c,*]

[a] School of Engineering, The University of Tokyo, Tokyo 113, Japan
[b] Vinyl Environmental Council, Tokyo 104, Japan
[c] Department of Forestry, National Chung Hsing University, Taichung 402, Taiwan

A B S T R A C T

Titanium dioxide (TiO_2) is the most essential additive in polyvinyl chloride (PVC) matrixes used for outdoor applications. In this study, we primarily investigate the effect of TiO_2 on the chemical and molecular changes in PVC sidings during QUV accelerated weathering. The results of this study show that carbonyl and polyene groups were generated on the surface of all of the specimens after 480 h of accelerated weathering but that loading TiO_2 into PVC successfully inhibited the increase in the number of these oxidative groups over the entire exposure period compared to PVC without TiO_2. In addition, a significant decrease in the number average molecular weight (M_n) and the formation of an insoluble gel were observed for PVC without TiO_2 after accelerated weathering. However, the time required for the M_n to decline increased with the amount of TiO_2 that was loaded into the PVC matrix, and no insoluble gel was observed during weathering. Furthermore, the crystallinity of PVC without TiO_2 increased noticeably after 1920 h of accelerated weathering, whereas no significant change was observed in the crystallinity of PVC with TiO_2. These results demonstrate that simultaneous chain scission and crosslinking reactions occurred in PVC without TiO_2, whereas only chain scission occurred in PVC containing TiO_2. In addition, the chain scission of PVC without TiO_2 was initiated earlier than for PVC with TiO_2, producing shorter and more mobile chains that underwent secondary crystallization. Accordingly, TiO_2 acted as a UV absorber and a radiation screener such that the probability of chain scission was reduced for TiO_2-loaded PVC sidings.

© 2014 Elsevier Ltd. All rights reserved.

1. Introduction

In 2011, 32.3 million tons of polyvinyl chloride (PVC) were used worldwide. PVC usage is predicted to reach approximately 49.53 million tons in 2020, corresponding to an annual average growth rate of 4.9% [1]. However, PVC use in Asia accounts for over half of the PVC products used worldwide [2]. After the addition of appropriate stabilizers, PVC can be applied in various fields, such as automobiles, aviation, civil construction and home and electronic appliances, etc. This polymer is an indispensable material for supporting our lifestyle and industrial infrastructure. In recent years, sustainable building construction has been the primary concern in the fields of civil engineering and architecture to maintain a sustainable society and protect the global environment. Therefore, appropriate building materials must be selected that are durable, recyclable and have low CO_2 emissions in consideration of the entire life cycle. In addition, the low cost and good weatherability of PVC products make this polymer very suitable for use in exterior applications in construction, such as windows, cladding structures and sidings, which are primarily used in North America. In particular, PVC use in exterior siding in new single-family houses accounted for approximately 36% of total PVC use in the USA in 2010 [3]. However, such PVC sidings suffer from degradation by various natural weathering factors, e.g., UV, heat and moisture.

However, PVC exterior materials used in practice contain additives such as calcium/zinc stearates, organotin mercaptide and inorganic UV absorbers that directly protect the material from degradation. TiO_2 is an inorganic UV absorber that is often used in PVC materials to prevent reaction with UV, humidity and oxygen by reducing the diffusion of electrons and positive holes to the reaction surface. Therefore, the surface becomes photo-oxidative and prone to photo-catalytic degradation because of the production of free radicals that accelerate degradation [4]. Many studies have

investigated the changes in the chemical and physical properties [5–8] and photo-oxidation mechanisms [6,9–14] of PVC films with and without additives under artificial weathering. Unfortunately, limited information is available on the physicochemical properties of PVC sidings with or without TiO_2 under QUV accelerated weathering. Thus, the aim of this work is to determine the effects of TiO_2 on the weathering properties of PVC sidings and to investigate physicochemical changes, including in chemical functional groups, the molecular weight distribution (MWD), the crystallinity and color changes, as a function of the exposure time.

2. Materials and methods

2.1. Materials

Compression-molded 0.5-mm thick PVC specimens (Kane Vinyl S1001) were supplied by Kaneka Co. (Japan). The PVC matrix contained additives that were similar to those used in outdoor applications of PVC sidings. The formulations used in the specimen are summarized in Table 1. These additives, which included acrylic polymer (Kane Ace PA-20, Kaneka, Japan), paraffin wax (Luvax-1266, Nippon Seiro, Japan), organotin mercaptide (TM-181 FS, Dow Chemical, USA) and fatty acid soap (calcium stearate and zinc stearate), are used as a processing aid, a lubricant, a thermal stabilizer and a HCl quencher, respectively. In addition, TiO_2 (R-105, DuPont, USA) is used as an inorganic pigment. In this study, the content of all of the additives was kept constant, except for TiO_2, which was added at contents of 0, 5 and 10 phr.

2.2. Accelerated weathering test

Accelerated weathering was conducted in a QUV tester using fluorescent lamps UVA-340 (Q-Lab, USA). The varying spectral energy distribution provided the best possible simulation of sunlight over the critical short wavelength region from 365 nm to the solar cutoff of 295 nm. The irradiance of the peak emission was 0.68 W/m^2 at 340 nm. This wavelength is significant in the accelerated degradation of PVC because PVC only absorbs irradiation from 310 to 370 nm [15]. The test cycle in this study consisted of 8 h of UV exposure at 50 ± 3 °C and 4 h in the dark with condensation at the same temperature. A complete test lasted 1920 h (80 days). All weathered specimens were air-dried in ambient conditions for 24 h before measuring various properties.

2.3. ATR-FTIR spectral measurements

The attenuated total reflectance Fourier transform infrared (ATR-FTIR) spectra of the PVC specimens were recorded using a Spectrum 100 FTIR spectrometer (PerkineElmer, UK) equipped with a MIRacle ATR accessory (Pike Technologies, USA). The spectra were collected by co-adding 32 scans at a resolution of 4 cm^{-1} over a 650 to 4000 cm^{-1} range.

Table 1
Specimen formulations in this study.

Ingredient	Chemical formula	Content (phr)		
		PVC(T$_0$)	PVC(T$_5$)	PVC(T$_{10}$)
PVC matrix	$(CH_2CHCl)_n$	100	100	100
Acrylic polymer	$(CH_2CCH_3COOCH_3)_n$	0.7	0.7	0.7
Paraffin wax	C_nH_{2n+2} ($n = 18$–48)	0.5	0.5	0.5
Organotin mercaptide	$R'_nSn(SCH_2COOR'')_{4-n}$	0.6	0.6	0.6
Fatty acid soap	$Ca(RCOO)_2$, $Zn(RCOO)_2$	1.5	1.5	1.5
Titanium dioxide	TiO_2	0	5	10

2.4. Gel permeation chromatography (GPC)

The number average molecular weight (M_n), the weight average molecular weight (M_w) and the MWD of the PVC specimens were measured using a GPC, which was equipped with a PU-2080 pump (Jasco, Japan), a RI-2031 refractive index detector (Jasco, Japan) and 10E3A/10E4A columns (Phenogel, USA). Tetrahydrofuran (THF) was used as the isocratic mobile phase at a flow rate of 1 mL/min. A series of polystyrene calibration standards was used to calculate M_n and M_w. Before sample injection, the specimens were dissolved in THF and then filtered through a 0.2-μm hydrophilic polypropylene (GHP) membrane to remove insoluble particles.

2.5. Gel content analysis

For determination of gel content, the weathered specimens were cut into pieces and immersed in THF for 24 h. In order to wash a gel completely free of soluble PVC, three extractions by the repeated centrifugation and decantation of a gel with fresh THF was used. The weight of the gel is determined after removal of THF by evaporation.

2.6. Differential scanning calorimetry (DSC) thermal analysis

The thermal properties of the PVC specimens were measured using a DSC-7 (PerkineElmer, UK). The samples (ca. 1 mg) were encapsulated in aluminum pans and heated from room temperature to 260 °C at a heating rate of 20 °C/min under a nitrogen flow (20 mL/min). The PVC crystallinity (X) was obtained as a function of the weathering time using the following expression: $X(\%) = \Delta H_{m(t)}/[\Delta H_m^0 \times W_p] \times 100$, where $\Delta H_{m(t)}$ denotes the melting enthalpy for the specimen at the weathering time t, ΔH_m^0 denotes the melting enthalpy of 100% crystalline PVC, and W_p denotes the weight percentage of the PVC in the samples. The ΔH_m^0 value has been estimated to range between 40 and 181 J/g [16]. In this study, we tool ΔH_m^0 to equal 176 J/g, which is the value obtained for fully crystalline PVC, as measured by TA instruments [17].

2.7. Surface color

The CIE $L^*a^*b^*$ color system on surface color of specimens after accelerated weathering were measured by a spectrophotometer (Minolta CM-3600d, Japan) under a D_{65} light source. Therein, L^* is the value on the white/black axis, a^* is the value on the red/green axis, b^* is the value on the yellow/blue axis and ΔE^* is the color difference ($\Delta E^* = [(\Delta L^*)^2 + (\Delta a^*)^2 + (\Delta b^*)^2]^{1/2}$).

2.8. Statistical analysis

All of the results were expressed in the form of a mean $\pm$ SD. The significance of difference was calculated using Scheffe's test, and P values < 0.05 were considered to be significant.

3. Results and discussion

3.1. FTIR analysis

FTIR-ATR was used to determine the changes in the functional groups on the surface of the specimens during accelerated weathering. The characteristic absorption bands of the PVC sidings were determined by separately measuring the components of the specimen, including the PVC matrix and each additive, before weathering. As expected, no absorption peak was found over the 1450–1750 cm^{-1} range in the PVC matrix spectrum [18]. In contrast, the fatty acid soaps (Ca/Zn stearates) exhibited significant

absorption peaks at 1473 cm^{-1} and 1578/1541 cm^{-1}, corresponding to the CH bending in CH$_2$ and the carboxylate (COO$^-$) stretching, respectively [19–21]. The peak at 1731 cm^{-1} (C=O) could be assigned to one of the specific functional groups in organotin mercaptide and the acrylic processing aid [22–24]. In the FTIR spectra of PVC containing TiO$_2$, TiO$_2$ absorption was observed below 700 cm^{-1}, and no significant differences were detected between the unweathered and weathered specimens. Table 2 shows the assignment of the specific bands for unweathered PVC(T$_0$). In addition to these absorption ranges, peaks for Ca/Zn stearates were observed within the 1450–1600 cm^{-1} range. These spectra could be easily subtracted during the aging process, enabling the changes in the specific functional groups to be quantified by periodic measurement of the variations in the absorbance.

Fig. 1A shows the FTIR-ATR spectra of PVC(T$_0$) after accelerated weathering for 1920 h. The wide range of the wavenumbers between 1450 and 3000 cm^{-1} was attributed to photochemical changes in the constituents of the PVC specimens. An increase in the absorbance of two bands at 1718 and 1630 cm^{-1} was observed, whereas the absorbances at 2917, 2850, 1578, 1541 and 1470 cm^{-1} decreased. Furthermore, to accurately observe the changes in the functional groups of PVC and the stabilizers, the overlapping spectra from 1450 to 1900 cm^{-1} were compared during the 1920 h of accelerated weathering. Fig. 1B shows that polyenes formed gradually at 1630 cm^{-1} after 120 h of exposure. A significant increase in the absorbance of the carbonyl groups also appeared at 1718 cm^{-1} after 480 h of exposure, which has been assigned to β-chlorocarboxylic acid by Gardette and Lemaire [12]. However, the absorption bands at 1745 and 1785 cm^{-1} corresponding to α,α,-dichloroketones and acid chloride were not distinguishable because of the overlap between the bands. In previous studies [25,26], the bands at 1718 cm^{-1} have been assigned to critical products resulting from main-chain scission that accumulated at a quasi-linear rate. Meanwhile, the Ca/Zn stearate absorption disappeared for all of the specimens after 480 h of exposure. Fig. 2 shows the absorbances for each specimen at 1630 and 1718 cm^{-1}. The absorbance at 1718 cm^{-1} increased with the weathering time for all of the PVC specimens and especially for PVC(T$_0$). After 1920 h of exposure, the absorbances of PVC(T$_0$), PVC(T$_5$) and PVC(T$_{10}$) were 3.9, 2.3 and 2.2, respectively. However, no obvious differences between PVC(T$_5$) and PVC(T$_{10}$) were observed. Meanwhile, the absorbance at 1630 cm^{-1} for PVC(T$_0$) ranged from 0.8 at 480 h up to 2.0 at 1440 h and remained constant up to 1920 h of exposure. In contrast, the absorbances of PVC(T$_5$) and PVC(T$_{10}$) were less than that of PVC(T$_0$) and fluctuated steadily over the exposure period. This result demonstrates that the specimen with TiO$_2$ effectively restrained the generation of carbonyl and polyene groups during
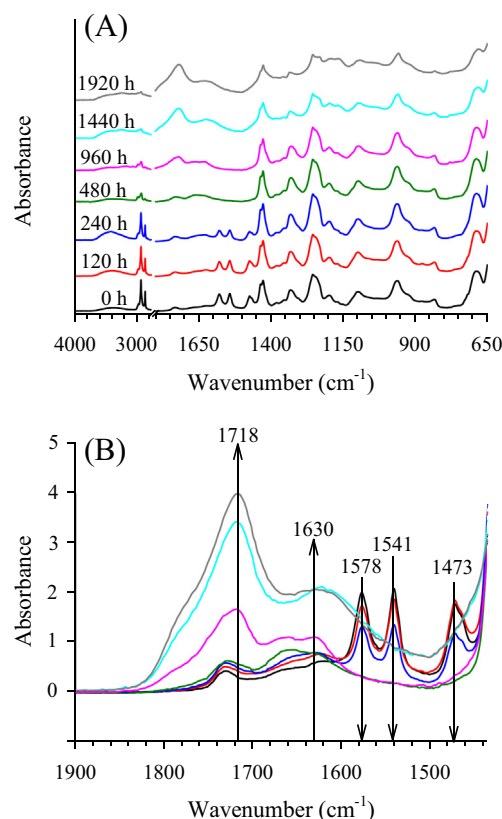
Fig. 1. FTIR-ATR spectra for PVC(T$_0$) over 1920 h of accelerated weathering for the following ranges: (A) 650–4000 cm^{-1} and (B)1435–1900 cm^{-1}.

accelerated weathering. Gardette and Lemaire [12] have reported a similar trend.

However, two processes governed the changes in the functional groups for all of the specimens before and after 480 h of exposure. Before 480 h of accelerated weathering, the Ca/Zn stearates and TiO$_2$ inhibited oxidation products for all of the specimens, but the bands assigned to the Ca/Zn stearates disappeared at 480 h. Thus, the Ca/Zn stearates may have been washed away by water or may have reacted with hydrogen chloride (a well-known product released by the photo-oxidation of PVC). After 480 h of exposure, the surfaces of all of the specimens had generated the oxidation reaction product; however, a relatively minor chemical change was observed for PVC with TiO$_2$. Thus, TiO$_2$ appears to have greatly suppressed the progression of photo-oxidation. Therefore, the

Table 2
Assignments for principle bands in unweathered PVC(T$_0$) spectra.

Wavenumber (cm^{-1})	Assignment	Reference
PVC matrix		
2968	C–H stretching of CHCl	[18]
2911	C–H stretching of CH$_2$	[18]
1435, 1426	CH$_2$ wagging	[18]
1097	C–C stretching	[18]
963	CH$_2$ rocking	[18]
690	C–Cl stretching	[18]
Additives		
2917, 2850	C–H stretching of CH$_2$ in paraffin wax	–
1731	C=O in organotin mercaptide and acrylic processing aid	[22–24]
1578	COO$^-$ (carboxylate) stretching in Ca stearate	[19–21]
1541	COO$^-$ (carboxylate) stretching in Zn stearate	[19–21]
1473	C–H bending of CH$_2$ in Ca/Zn stearates	[19–21]
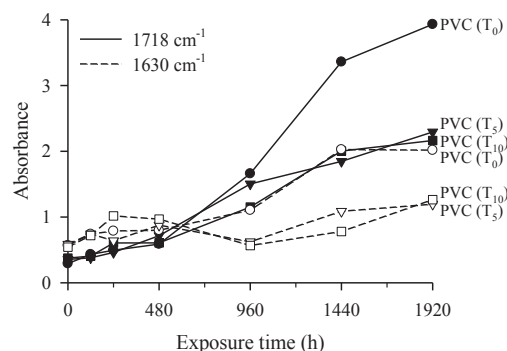
Fig. 2. Absorbances of various specimens at 1718 and 1630 cm^{-1} after accelerated weathering for 1920 h.

combined use of Ca/Zn stearates and TiO_2 resulted in a synergistic effect that significantly reduced photo-degradation.

3.2. Molecular weight changes

In the previous section, we confirmed that carbonyl and polyene groups were generated on the surface of PVC sidings with or without TiO_2 after accelerated weathering. We also suggested that the molecular weight changed after weathering because of the photo-degradation of PVC by chain scission or because of crosslinking [8]. Therefore, GPC analysis was used in this study to determine the changes in the macromolecular sizes of the PVC sidings during accelerated weathering. The number average molecular weight was calculated quantitatively using polystyrene as a standard (see Table 3). The results show that the M_n of PVC(T_0) started decreasing at 480 h of exposure, had decreased by approximately 15% (64.2 kg/mol) at 960 h and then leveled off. However, the M_n value only decreased by 12% (67.5 kg/mol) for PVC(T_5) at 1440 h and by 13% (69.7 kg/mol) for PVC(T_{10}) at 1920 h. As expected, there was a greater decrease in the M_n of PVC(T_0) than that of PVC(T_5) and PVC(T_{10}). This result also shows that chain scission was inhibited by increasing the loading amount of TiO_2 in the PVC matrix. The changes observed in the weight average molecular weight were insignificant for all of the specimens after accelerated weathering. However, the formation of a gel, which was insoluble in THF, was observed in PVC(T_0) after 960 h of accelerated weathering and corresponded to a product with 3-dimensional crosslinks. The gel content was found to be 7.9, 10.5 and 10.3% at exposure time of 960, 1440 and 1920 h, respectively. In contrast, both PVC(T_5) and PVC(T_{10}), excluded TiO_2, dissolved completely in THF over the entire exposure time. These results show that chain scission and crosslinking reactions occurred simultaneously in PVC without TiO_2 under accelerated weathering but that only chain scission occurred in PVC containing TiO_2. Table 4 shows the polydispersity index (PDI, M_w/M_n) of all specimens after accelerated weathering for 1920 h. A PDI range of approximately 1.7—2.0 was observed for all of the specimens. The PDI for PVC(T_0) increased significantly from an initial value of 1.77 up to 2.06 after accelerated weathering for 480 h and then increased slightly to 2.12 at 1920 h. The MWD also broadened with the exposure time. In contrast, no significant difference was observed between the PDI values of PVC(T_5) and PVC(T_{10}) after accelerated weathering. David et al. [27] reported only decreases in the M_n and M_w values from main-chain scission in the absence of crosslinking. When chain scission and crosslinking occur simultaneously, and the probability of chain scission is less than that of crosslinking, the PDI increases and an insoluble fraction appears. This mechanism can describe the change in the molecular weight of PVC(T_0) after accelerated weathering. Although a reduction in the M_n value was observed for PVC(T_5) and PVC(T_{10}), there was no significant change in the M_w value after accelerated weathering. This behavior can be explained

Table 4
Polydispersity indexes (PDIs) for various specimens after accelerated weathering over 1920 h.

Exposure time (h)	PDI (M_w/M_n)		
	PVC(T_0)	PVC(T_5)	PVC(T_{10})
0	1.77 ± 0.04[C]	1.76 ± 0.13[B]	1.81 ± 0.07[AB]
120	1.81 ± 0.02[C]	1.86 ± 0.10[B]	1.82 ± 0.03[AB]
240	1.92 ± 0.12[BC]	1.92 ± 0.05[AB]	1.82 ± 0.06[AB]
480	2.06 ± 0.09[AB]	1.92 ± 0.05[AB]	1.77 ± 0.01[AB]
960	2.07 ± 0.06[AB]	1.90 ± 0.07[AB]	1.80 ± 0.03[AB]
1440	2.17 ± 0.09[A]	1.96 ± 0.07[A]	1.82 ± 0.03[AB]
1920	2.12 ± 0.09[AB]	1.92 ± 0.03[AB]	1.91 ± 0.04[A]

Values are presented in the form of a mean ± SD (n = 5); different letters indicate significant differences among groups at different exposure times ($P < 0.05$).

by attributing the increase in the M_w value primarily to crosslinking from the formation of dialkylperoxide bridges from oxidation products or free radical bridges from polyenes [28]; however, this reaction would have been inhibited by the TiO_2 contained in PVC(T_5) and PVC(T_{10}). The FTIR-ATR spectra also confirmed that the intensity of the carbonyl and polyene peaks for PVC with TiO_2 were smaller than for PVC without TiO_2. Moreover, Gardette and Lemaire [12] reported that oxidation was limited to within 80 μm from an irradiated surface of PVC with a loading of 8% TiO_2, whereas a 150 μm oxidation profile and a remarkable change in the molecular weight were observed for PVC without TiO_2. Fig. 3 shows the MWD of PVC sidings with various amounts of TiO_2 after accelerated weathering. Fig. 3A clearly shows time-dependent increases in both the lower and higher molecular weight fractions of the MWD of PVC(T_0). This result provided further evidence of simultaneous chain scission and crosslinking reactions in PVC(T_0) after accelerated weathering. However, the MWD of PVC(T_5) and PVC(T_{10}) was mostly shifted to lower molecular weights after accelerated weathering, especially for PVC(T_{10}) (see Fig. 3B—C). This result indicates that chain scission was the predominant mechanism in PVC loaded with TiO_2. Similar results were obtained by Rabinovitch et al. [8].

3.3. Crystallinity

Many studies [29—32] have been conducted on how PVC crystallinity changes during heat treatment or thermal aging using the DSC method. However, very few studies to date have investigated the crystallinity of an amorphous polymer in a weathering environment using DSC. In this study, chain scission in all of the specimens was determined by molecular weight measurements, thereby verifying whether the crystallinity was generated by molecular rearrangement after accelerated weathering. Fig. 4 shows the heat flow in PVC(T_0) for various exposure times. Heat flow was observed in PVC(T_0) over a wide temperature range of 100—240 °C, within which two distinct α and β endotherm peaks appeared. It is

Table 3
Number average molecular weight (M_n) and gel content of various specimens after accelerated weathering for 1920 h.

Exposure time (h)	PVC(T_0)		PVC(T_5)		PVC(T_{10})	
	M_n (kg/mol)	Gel content (%)	M_n (kg/mol)	Gel content (%)	M_n (kg/mol)	Gel content (%)
0	76.4 ± 1.6[A]	—[a]	75.9 ± 3.3[A]	—	79.5 ± 3.9[A]	—
120	76.9 ± 0.6[A]	—	73.7 ± 2.0[AB]	—	79.6 ± 3.0[A]	—
240	75.4 ± 2.6[A]	—	74.1 ± 2.8[AB]	—	78.9 ± 3.6[A]	—
480	71.7 ± 1.9[AB]	—	74.1 ± 2.7[AB]	—	81.6 ± 1.0[A]	—
960	64.2 ± 3.4[C]	7.9	74.2 ± 2.8[AB]	—	77.2 ± 1.3[AB]	—
1440	65.3 ± 3.0[BC]	10.5	67.5 ± 1.9[B]	—	79.7 ± 3.4[A]	—
1920	66.4 ± 2.9[BC]	10.3	68.8 ± 1.6[B]	—	69.7 ± 2.5[B]	—

Values are presented in the form of a mean ± SD (n = 5); different letters indicate significant differences among groups at different exposure times ($P < 0.05$).
[a] Not detected.
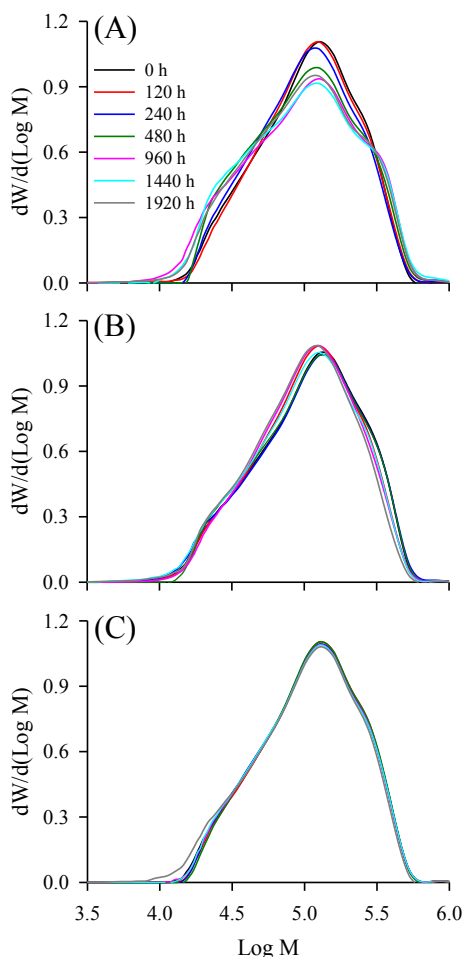
Fig. 3. Molecular weight distribution of various specimens over 1920 h of accelerated weathering: (A) PVC(T_0), (B) PVC(T_5) and (C):PVC(T_{10}).

well-known that the endothermic α (100–210 °C) peak can be attributed to the melting of material that initially melted during compression molding and then recrystallized upon cooling, whereas the β (210–240 °C) peak can be attributed to the melting of material that had not previously melted during compression molding [29–31]. Fig. 4 shows that the area under the endothermic α peak increased significantly with the exposure time. The area under the endothermic α peak appeared to be related to the level of fusion in the material. This result may indicate that crystallizable segments subsequently recrystallized to produce many smaller or
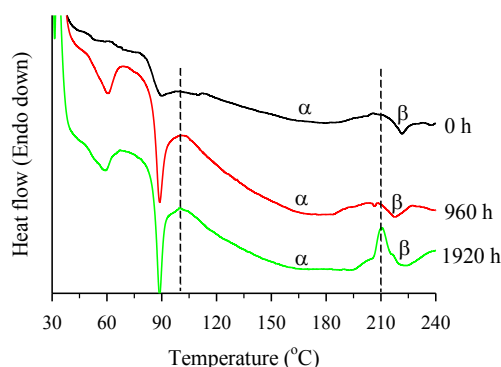
Fig. 4. DSC curves for PVC(T_0) after accelerated weathering for 0 h, 960 h and 1920 h.

lower melting crystallites on the PVC surface [32]. Similar results have been observed for other polyolefins during accelerated weathering [33]. Additionally, for the weathered PVC(T_0), two sharp endothermic peaks were observed at around 60 °C and 90 °C in Fig. 4. For the former peak, it would be the melting of stearic acid, which was formed from the reactions of metal stearates with HCl released by dehydrochlorination after accelerated weathering. This result consists with Sari and Kaygusuz [34] who reported that the melting temperature of 64.7 °C was measured in PVC/stearic acid blends. In contrast, this peak was not observed for PVC with TiO_2 specimens during the entire exposure period. Furthermore, heat flow exhibited a remarkable endothermic peak at around 90 °C in all specimens after weathering. This peak may belong to the melting of crystals formed from additives during weathering period and further investigations are required to clarify which crystals and reactions have occurred. On the other hand, Fig. 5 shows the degree of the crystallinity for various PVC sidings. The crystallinity of all of the specimens decreased in the first 960 h of accelerated weathering. Once the exposure time exceeded 960 h, the PVC(T_0) crystallinity noticeably increased from its initial value of 4% to 13–14% after 1440–1920 h of exposure, whereas no significant changes were observed in the crystallinities of PVC(T_5) and PVC(T_{10}) during this period. This result indicates that chain scission in PVC(T_0) was initiated earlier than for the other specimens, producing shorter and more mobile chains that could undergo secondary crystallization. In contrast, a slight chain scission was only observed after 1440 and 1920 h of exposure time for PVC(T_5) and PVC(T_{10}), respectively (Table 4). This result demonstrates that TiO_2 acted as a UV absorber and a radiation screener to reduce the probability of chain scission and inhibit the penetration of UV beyond the surface layer deeper into the specimen.

3.4. Color changes

Color measurement provides a degree of photodegradation of polymer during weathering. The mechanism of color change is always related to a competition between varying chain length of polyenes and photobleaching [12,35]. The data in Fig. 6 indicated that effect of TiO_2 on color variation of PVC sidings during the 1920 h of accelerated weathering. The ΔE^* values of all specimens generally increased with increasing exposure time (Fig. 6A). However, the ΔE^* of PVC(T_0) exhibited an immediate increase in the first 24 h, and then increased significantly to 27.9 at 1920 h. In contrast, the ΔE^* values of PVC(T_5) and PVC(T_{10}) increased gradually to 4.3 and 2.6 after 240 h of exposure, respectively, and both remained constant up to 1920 h. These results demonstrated that the color
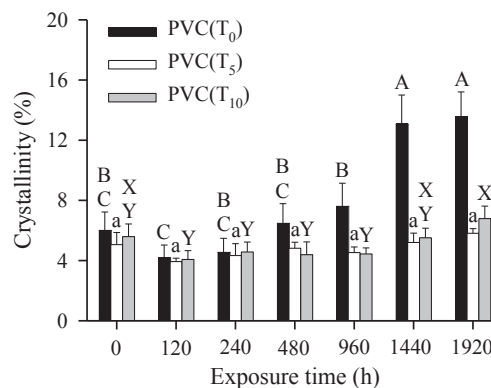
Fig. 5. Changes in crystallinity for various specimens over 1920 h of accelerated weathering: the results are presented in the form of a mean ± SD ($n = 5$), and different letters indicate significant differences among groups at different exposure times ($P < 0.05$).
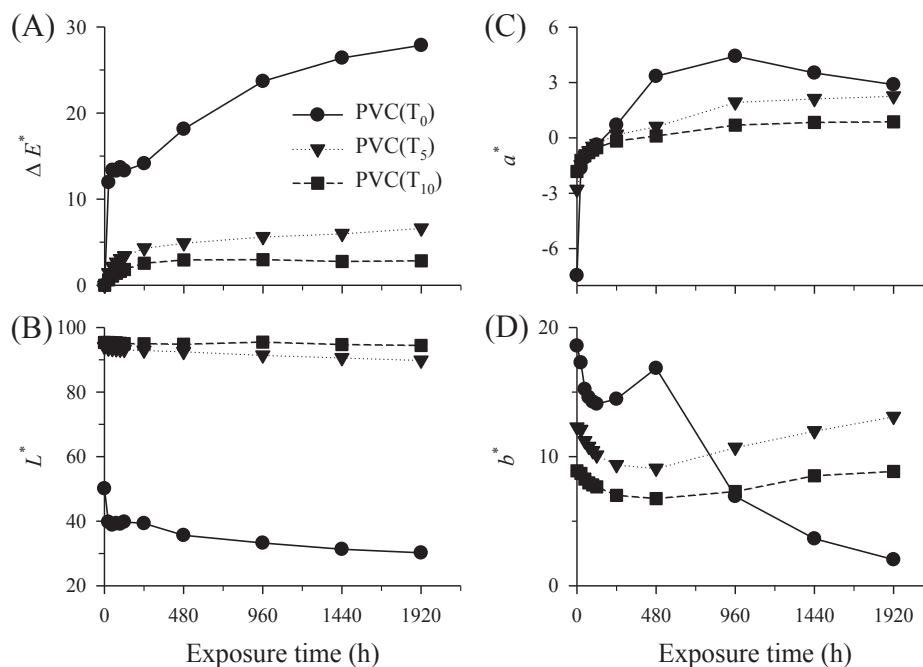
Fig. 6. Effect of titanium dioxide on ΔE^* (A), L^* (B), a^* (C) and b^* (D) values of various specimens after accelerated weathering for 1920 h. Mean values are shown ($n = 5$).

difference (ΔE^*) of TiO_2-loaded PVCs was lower than that of PVC without TiO_2. A similar tendency was reported by Matuana et al. [36]. This observation implied that the presence of TiO_2 in PVC matrix provided color stabilization during accelerated weathering. Fig. 6B shows the L^* value of PVC(T$_0$) ($L^* = 50.1$) was remarkably lower than that of PVC(T$_5$) ($L^* = 94.1$) and PVC(T$_{10}$) ($L^* = 95.4$) at 0 h because of TiO_2 as a white pigment to give the PVCs with high lightness. After accelerated weathering, there were no significant changes for the L^* of PVC containing TiO_2. However, the L^* value of PVC(T$_0$) decreased significantly during weathering, particularly in the first 24 h. Furthermore, Fig. 6C shows the a^* value of PVC(T$_0$) increased sharply from an initial value of -7.5 to 3.3 ($\Delta a^* = 10.8$) after 480 h of exposure. However, the PVC(T$_{10}$) exhibited only a little variation during the 1920 h of exposure ($\Delta a^* < 3$). Finally, the b^* value of PVC(T$_0$) was decreasing dramatically at the period of 480 h ($b^* = 16.9$) to 1920 h ($b^* = 2.0$), but the b^* values of TiO_2-loaded PVCs had no significant differences during the exposure period. The Δb^* values of PVC(T$_5$) and PVC(T$_{10}$) were 0.8 and -0.1 after 1920 h of exposure, respectively. According to the results mentioned above, the surface color of TiO_2-loaded PVCs, especially for high-loading TiO_2, remained whiter than PVC(T$_0$) after accelerated weathering, which was similar to that reported by Edge et al. [37]. Accordingly, the loading amount of TiO_2 was an important factor on polymer stabilization during weathering. The higher loading amount of TiO_2 in PVC matrix, the higher has the stability against weathering.

4. Conclusions

Simultaneous chain scission and crosslinking reactions played a crucial role in the QUV accelerated weathering of PVC sidings without TiO_2. Chain scission produced shorter and more mobile molecules that were able to undergo secondary crystallization, thereby increasing the PVC crystallinity after weathering. However, adding TiO_2 to PVC effectively inhibited photo-oxidation and chain scission and improved the weatherability of PVC because the TiO_2 acted as a good UV screener and absorber in the PVC matrix. These results implied that TiO_2-loaded PVC sidings should be able to retain their mechanical properties more effectively during outdoor weathering. Thus, the effect of TiO_2 on the surface morphology and the mechanical properties of PVC sidings for outdoor applications should be investigated in future studies.

References

[1] GBI research. Polyvinyl chloride (PVC) global market to 2020 – growth from Asia-Pacific construction, packaging and electrical sectors continues to drive demand http://www.giiresearch.com/report/gbi249114-polyvinyl-chloride-pvc-global-market-growth-from.html; August 22, 2012.

[2] Ministry of Economy, Trade and Industry. Forecast of global supply and demand trends for petrochemical products http://www.vec.gr.jp/lib/lib2_5.html; April 30, 2013.

[3] U.S. Census Bureau. Principle type of exterior cladding comparison new one-family houses sold http://www.census.gov/const/C25Ann/sftotalexwallmat.pdf; 2010.

[4] Day RE. The role of titanium dioxide pigments in the degradation and stabilisation of polymers in the plastics industry. Polym Degrad Stabil 1990;29(1):73–92.

[5] Decker C, Balandier M. Degradation of poly(vinyl chloride) by U.V. radiation-I. Kinetics and quantum yields. Eur Polym J 1982;18(12):1085–91.

[6] Anton-Prinet C, Mur G, Gay M, Audouim L, Verdu J. Photoageing of rigid PVC—I. Films containing CaZn thermal stabilizer. Polym Degrad Stabil 1998;60(2–3):265–73.

[7] DeCoste JB, Howard J, Wallder V. Weathering of poly(vinyl chloride). Effect of composition. Ind Eng Chem Chem Eng Data Ser 1958;3(1):131–40.

[8] Rabinovitch EB, Summers JW, Northcott WE. Changes in properties of rigid PVC during weathering. J Vinyl Technol 1993;15(4):214–8.

[9] Decker C. Degradation of poly(vinyl chloride) by U.V. radiation-II. Mechanism. Eur Polym J 1984;20(2):149–55.

[10] Gardette JL, Lemaire J. Wavelength effects on the photo-chemistry of poly(vinyl chloride). Polym Degrad Stabil 1986;16(2):147–58.

[11] Gardette JL, Gaumet S, Lemaire J. Photooxidation of poly(vinyl chloride). 1. A reexamination of the mechanism. Macromolecules 1989;22(6):2576–81.

[12] Gardette JL, Lemaire J. Photo-oxidation of poly(vinyl chloride): part 3-Influence of photo-catalytic pigments. Polym Degrad Stabil 1991;33(1):77–92.

[13] Gardette JL, Lemaire J. Photothermal and thermal oxidations of rigid, plasticized and pigmented poly(vinyl chloride). Polym Degrad Stabil 1991;34(1–3):135–67.

[14] Anton-Prinet C, Mur G, Gay M, Audouin L, Verdu J. Change of mechanical properties of rigid poly(vinylchloride) during photochemical ageing. J Mater Sci 1999;34(2):379–84.

[15] Dekker M, editor. Handbook of polymer degradation. New York: INC; 1992.

[16] Komoroski RA, Lehr MH, Goldstein JH, Long RC. Solid-state deuterium nuclear magnetic resonance of crystallinity in poly(vinyl chloride). Macromolecules 1992;25(13):3381–4.

[17] Blaine RL. Polymer Heats of Fusion. TA instruments. TN048.

[18] Beltrán M, Marcilla A. Fourier transform infrared spectroscopy applied to the study of PVC decomposition. Eur Polym J 1997;33(7):1135−42.
[19] Benavides R, Edge M, Allen NS. The mode of action of metal stearate stabilisers in poly(vinyl chloride). I. Influence of pre-heating on melt complexation. Polym Degrad Stabil 1994;44(3):375−8.
[20] Wang M, Xu J, Wu H, Guo S. Effect of pentaerythritol and organic tin with calcium/zinc stearates on the stabilization of poly(vinyl chloride). Polym Degrad Stabil 2006;91(9):2101−9.
[21] Atek D, Belhaneche-Bensemra N. FTIR investigation of the specific migration of additives from rigid poly(vinyl chloride). Eur Polym J 2005;41:707−14.
[22] Burley JW. Mechanistic aspects of the thermal stabilisation of PVC by organotin compounds. Appl Organomet Chem 1987;1:95−113.
[23] Balköse D, Arkış E. Thermal stabilisation of poly(vinyl chloride) by organotin compounds. Polym Degrad Stabil 2005;88:46−51.
[24] Garcia D, Black J. Fourier infrared micro spectroscopy mapping. Applications to the vinyl siding industry. J Vinyl Addit Technol 1997;3(3):200−4.
[25] Gardette JL, Lemaire J. Prediction of the long-term outdoor weathering of poly(vinyl chloride). J Vinyl Technol 1993;15(2):113−7.
[26] Lemaire J, Lacoste J, Siampiringue N. Proceedings 8th International Symposium on Weatherability22; 2010. pp. 50−7.
[27] David C, Trojan M, Daro A. Photodegradation of polyethylene: comparison of various photoinitiators in natural weathering conditions. Polym Degrad Stabil 1992;37(3):233−45.
[28] Anton-Prinet C, Dubois J, Mur G, Gay M, Audouim L, Verdu J. Photoageing of rigid PVC-II. Degradation thickness profiles. Polym Degrad Stabil 1998;60(2−3):275−81.
[29] Tsitsilianis C, Tsapatsis M, Economou Ch. Effects of crystallinity on ageing phenomena in poly(vinyl chloride). Polymer 1989;30(10):1861−6.
[30] Dawson PC, Gilbert M, Maddams WF. Comparison of X-ray diffraction and thermal analysis methods for assessing order in poly(vinyl chloride). J Polym Sci Pt B-Polym Phys 1991;29(11):1407−81.
[31] Gilbert M, Vyvoda JC. Thermal analysis technique for investigating gelation of rigid PVC compounds. Polymer 1981;22(8):1134−6.
[32] Gilbert M, Ansari KE. Structure−property relationships in PVC compression moldings. J Appl Polym Sci 1982;27(7):2553−61.
[33] Jabarin SA, Lofgren EA. Photooxidative effects on properties and structure of high-density polyethylene. J Appl Polym Sci 1994;53:411−23.
[34] Sari A, Kaygusuz K. Studies on poly(vinyl chloride)/fatty blends as shape-stabilized phase change material for latent heat thermal energy storage. Indian J Eng Mater Sci 2006;13(3):253−8.
[35] Bacaloglu R, Stewen U. Study of PVC degradation using a fast computer scanning procedure. J Vinyl Addit Technol 2001;7(3):149−55.
[36] Matuana LM, Kamdem DP, Zhang J. Photoaging and stabilization of rigid PVC/Wood-Fiber composites. J Appl Polym Sci 2001;80(11):1943−50.
[37] Edge M, Liauw CM, Allen NS, Herrero R. Surface pinking in titanium dioxide/lead stabilizer filled PVC profiles. Polym Degrad Stabil 2010;95(10):2022−40.